Journal of Hazardous Materials 186 (2011) 396–400

Contents lists available at ScienceDirect

Journal of Hazardous Materials

journal homepage: www.elsevier.com/locate/jhazmat

A numerical study on the thermal initiation of a confined explosive in 2-D geometry

Erdoğan Aydemir[a,1], Abdullah Ulas[b,*]

[a] TÜBİTAK-SAGE, PK 16 Mamak, 06261 Ankara, Turkey
[b] Middle East Technical University, 06531 Ankara, Turkey

ARTICLE INFO

Article history:
Received 31 August 2010
Received in revised form 26 October 2010
Accepted 4 November 2010
Available online 12 November 2010

Keywords:
Insensitive munitions
Slow cook-off
Fast cook-off
Ignition time
Ignition temperature
Explosive

ABSTRACT

Insensitive munitions design against thermal stimuli like slow or fast cook-off has become a significant requirement for today's munitions. In order to achieve insensitive munitions characteristics, the response of the energetic material needs to be predicted against heating stimuli. In this study, a 2D numerical code was developed to simulate the slow and fast cook-off heating conditions of confined munitions and to obtain the response of the energetic materials. Computations were performed in order to predict the transient temperature distribution, the ignition time, and the location of ignition in the munitions. These predictions enable the designers to have an idea of when and at which location the energetic material ignites under certain adverse surrounding conditions. In the paper, the development of the code is explained and the numerical results are compared with available experimental and numerical data in the literature. Additionally, a parametric study was performed showing the effect of dimensional scaling of munitions and the heating rate on the ignition characteristics.

1. Introduction

Thermal Initiation Theory describes the initiation of deflagration due to thermal effects from surrounding conditions and the heat generated inside the energetic material. Energetic materials are unstable and decompose rapidly as their temperature is raised. These materials can be characterized by a rough estimation of the ignition temperature. However, more accurate prediction of the ignition temperature depends on the size and shape of the energetic material and the rate at which it is heated.

Studies for the description of the Thermal Initiation Theory date back to 1920s. Semenov [1] made the uniform temperature distribution assumption in the energetic material with zero order reaction kinetics. This was the origin of the thermal explosion studies. However, this theory was only applicable for uniform temperature systems like well stirred liquids. Since uniform temperature distribution assumption does not well suit for solid energetic materials, Frank-Kamenetskii [2] proposed a theory based on the conductive heat transfer in the energetic material which allows time dependent temperature distribution prediction. Numerical studies on the ignition times and temperatures for energetic materials have been performed starting from 1960s. Zinn and Mader [3] applied Fourier series spatial representation for the solution to the reactive heat conduction equation to obtain ignition times for explosive material. Merzhanov and Abramov [4] used finite difference method for one-dimensional reactive heat conduction with the zero-order kinetic model. Anderson [5] developed the code TEPLO using finite difference method, which introduced temperature dependent material properties into the computations. Suceska [6] used finite difference method and developed code THERMEX for the solution of the reactive heat conduction equation problem with the zero-order kinetic model. This model has been modified to investigate the influence of different thermal decomposition kinetic models on the numerical modeling of self-ignition of propellants [7,8] and explosives under strong confinement [9]. Isler and Kayser [10] and McGuire and Tarver [11,12] used kinetic models such as power law model to predict the ignition behavior of various energetic materials.

Fast and slow cook-off threats are the two of the stimuli which the munitions may face during their life cycle. Against such undesired heating stimuli, measures are developed during design stage like applications of insulation, pressure release and mitigation. At this design stage, it is very useful to predict the time, temperature, and location of the ignition of an energetic material. The previous literature supplies valuable information on how to predict the ignition times of an energetic material with computations in a 1D domain representing simple geometries. However, detailed 2D analyses are necessary which enables the temporal and spatial

* Corresponding author. Tel.: +90 312 210 5260; fax: +90 312 210 2536.
E-mail address: aulas@metu.edu.tr (A. Ulas).
[1] Present address: Department of Engineering, University of Cambridge, CB2 1PZ Cambridge, United Kingdom.

0304-3894/$ – see front matter © 2010 Elsevier B.V. All rights reserved.
doi:10.1016/j.jhazmat.2010.11.015

characteristics of ignition which is applicable for more complex realistic munition geometries. Therefore, in this study, a computer code named REACON, which solves reactive heat conduction equation in order to predict the transient temperature distribution, the ignition time, and the location of ignition of an energetic material in a 2D computational domain is developed in FORTRAN language using finite element method.

2. Modeling and validation

The balance between the heat conduction, the accumulation, and the generation according to zero order kinetic law can be formulated by the very well known diffusion equation given in Eq. (1) [3,6].

$$\rho c\frac{\partial T}{\partial t} = k\nabla^2 T + \rho Q A e^{(-E/RT)} \tag{1}$$

$$0 = \sum_{j=1}^{n}\left[\begin{array}{l}\left(\displaystyle\int_{\Omega^e}(b\psi_i^e\psi_j^e)dxdy\right)\frac{dT_j^e}{dt}\\ +\left(\displaystyle\int_{\Omega^e}\left[\frac{d\psi_i^e}{dx}\left(a_{11}\frac{d\psi_j^e}{dx}+a_{12}\frac{d\psi_j^e}{dy}\right)+\frac{d\psi_i^e}{dy}\left(a_{21}\frac{d\psi_j^e}{dx}+a_{22}\frac{d\psi_j^e}{dy}\right)\right]dxdy\right)T_j^e\\ -\displaystyle\int_{\Omega^e}f\psi_i^e dxdy-\oint_{\Gamma^e}q_n\psi_i^e ds\end{array}\right] \tag{8}$$

In this equation, ρ is the density, c the heat capacity, T the temperature, t the time, k the thermal conductivity, Q the heat of decomposition, A the pre-exponential constant, E the activation energy, and R the gas constant. In Eq. (1), the term on the left hand side determines the time dependent heat accumulation. The first term on the right hand side is the diffusion term while the second term is related to the chemical heat release in the energetic material.

2.1. Finite element formulation

In order to achieve the finite element formulation of the problem, the two-dimensional diffusion equation can be expressed in the model differential equation form as given in Eq. (2).

$$b\frac{\partial T}{\partial t}-\frac{\partial}{\partial x}\left(a_{11}\frac{\partial T}{\partial x}+a_{12}\frac{\partial T}{\partial y}\right)-\frac{\partial}{\partial y}\left(a_{21}\frac{\partial T}{\partial x}+a_{22}\frac{\partial T}{\partial y}\right)-f=0 \tag{2}$$

In this equation a and b constants are functions of x and y and can be modified for 2D Cartesian, cylindrical, and spherical coordinates. Similarly, the heat generation term, f is temperature dependent and can be estimated by the appropriate kinetic model. In this study, *zero-order kinetic model* is used and the temperature dependent heat generation term is as given in Eq. (3).

$$f(T) = \rho\cdot Q\cdot A\cdot e^{(-E/RT)} \tag{3}$$

Firstly, for the finite element solution of the given model differential equation, the weak form of the equation for an element e is obtained as given in Eq. (4) where F_1 and F_2 are given in Eq. (5).

$$\int_{\Omega^e} w\left[b\frac{\partial T}{\partial t}-\frac{\partial}{\partial x}F_1-\frac{\partial}{\partial y}F_2-f\right]dxdy=0 \tag{4}$$

$$F_1 = a_{11}\frac{\partial T}{\partial x}+a_{12}\frac{\partial T}{\partial y}\quad F_2 = a_{21}\frac{\partial T}{\partial x}+a_{22}\frac{\partial T}{\partial y} \tag{5}$$

By applying integration by parts to the second order differential terms in Eq. (4) this equation takes the form given in Eq. (6).

$$0=\int_{\Omega^e}\left[wb\frac{\partial T}{\partial t}+F_1\frac{\partial w}{\partial x}+F_2\frac{\partial w}{\partial y}-fw\right]dxdy-\oint_{\Gamma^e}w(F_1\hat{n}_x+F_2\hat{n}_y)ds \tag{6}$$

For the finite element solution of the above equation, shape (Lagrange interpolation) functions are introduced for the element e with n nodes as shown in Eq. (7). Eq. (8) is obtained by defining differentials of T in terms of shape functions $\psi_i(x)$, selecting weight functions w equal to shape functions and rearranging the terms in Eq. (6).

$$T^e=\sum_{j=1}^{n}T_j^e\psi_j^e(x,y) \tag{7}$$

Each integral term in Eq. (8) forms matrices in sizes of number of nodes of that element and it can be symbolically expressed in terms of mass and stiffness matrices and temperature and force vectors as given in Eq. (9).

$$\left[M^e\right]\left\{\dot{T}^e\right\}+\left[K^e\right]\left\{T^e\right\}=\left\{f^e\right\} \tag{9}$$

After obtaining this system of equations for each element, matrices can be assembled for total number of elements and solution for the assembled system supplies the unknown temperature values. Differentiating $\left\{\dot{T}^e\right\}$ term using an α-family scheme leads to Eq. (10).

$$(1-\alpha)\left\{\dot{T}\right\}_s+\alpha\left\{\dot{T}\right\}_{s+1}=\frac{\left\{T\right\}_{s+1}-\left\{T\right\}_s}{\Delta t} \tag{10}$$

For the values of $\alpha=0$, $\alpha=1$, and $\alpha=0.5$, forward, backward, and Crank-Nicholson differencing schemes are obtained respectively. Applying this scheme to Eq. (9), Eq. (11) is obtained.

$$\begin{aligned}\left([M^e]+\alpha\Delta t[K^e]_{s+1}\right)\left\{T^e\right\}_{s+1} &= ([M^e]-(1-\alpha)\Delta t[K^e]_s)\left\{T^e\right\}_s\\ &+\Delta t\left(\alpha\left\{f^e\right\}_{s+1}+(1-\alpha)\left\{f^e\right\}_s\right)\end{aligned} \tag{11}$$

After defining the solution domain and material parameters and applying initial and boundary temperature conditions for the specified problem, an implicit procedure is followed for the solution of the system of equations given in Eq. (11). For the computation of the above given system of equations REACON (REActive CONduction) computer code is developed in FORTRAN language.

2.2. Code validation

Validation of the REACON code was performed by comparison of the calculated ignition times for a high explosive RDX sphere at different constant temperature boundary conditions with 1D version of REACON code and the values obtained from literature. Ignition time step can be defined in terms of the time rate of the

Table 1
Kinetic and thermo-physical material parameters of RDX.

ρ	1800 kg/m^3
c	2.093 kJ/kg K
k	0.293 W/m K
Q	2093 kJ/kg
A	3.16×10^{18} s^{-1}
E	199 kJ/mol

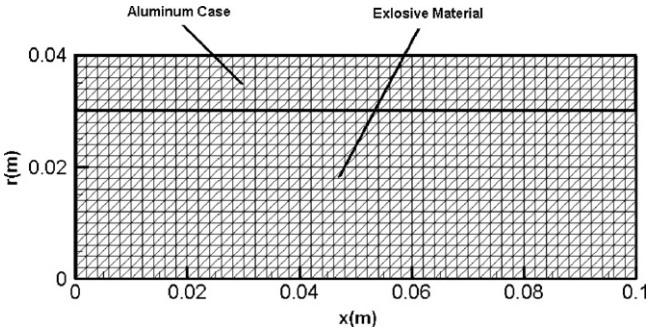

Fig. 1. Solution domain for the validation of REACON computational results with FLUENT.

temperature increase in the energetic material. In this study, ignition time step corresponds to the 5% larger temperature increase rate from the previous time step. For a 25.4 mm RDX sphere, 1D computations are performed in order to obtain the ignition times of this material at different constant temperature boundary conditions and the results are compared to the data from literature [3,5,6]. Same kinetic parameters and thermo-physical properties for RDX given in the referenced studies were used for consistency (Table 1). The comparison of the computed ignition times is presented in Table 2. A good agreement can be observed between the results obtained for the ignition times of RDX sphere at different constant temperature boundary conditions.

After having validated the code results in 1D transient case, a transient reactive conduction computation in a 2D axisymmetric cylindrical domain has been compared to a solution obtained by the commercial code FLUENT [13]. The solution domain with the generated mesh to be used by the REACON and the FLUENT codes is given in Fig. 1 with 2000 number of triangular elements. The boundary condition applied on this axial symmetric problem is increasing surface temperature at 200 K/h rate with an initial condition of 300 K. Planar symmetry boundary conditions were applied at each side of the domain. The material parameters for the aluminum and the explosive material (PBXN-110) used in the computations are provided in Table 3.

The plot of the temperature values during heating of the material at the specified locations in x and r coordinates A(0.05, 0.00), B(0.05,0.02) and C(0.05,0.03) is given in Fig. 2. A good agreement of the results is noticed from this figure. The validation of the REACON code was completed regarding the comparison of the results obtained for 1D and 2D transient solution of the conduction equation with heat generation. Therefore it can be concluded

Table 3
Material parameters used in the computations.

Material property	Values	
	Aluminum	PBXN-110
Density (kg/m^3)	2720	1670
Specific Heat (J/kg/K)	871	1465
Thermal Conductivity (W/m/K)	203	0.418
Heat of decomposition (J/kg)	–	1,842,200
Pre-exponential factor (1/s)	–	2.48×10^{18}
Activation energy (J/mol)	–	215,560
Universal gas constant (J/mol/K)	–	8.3145

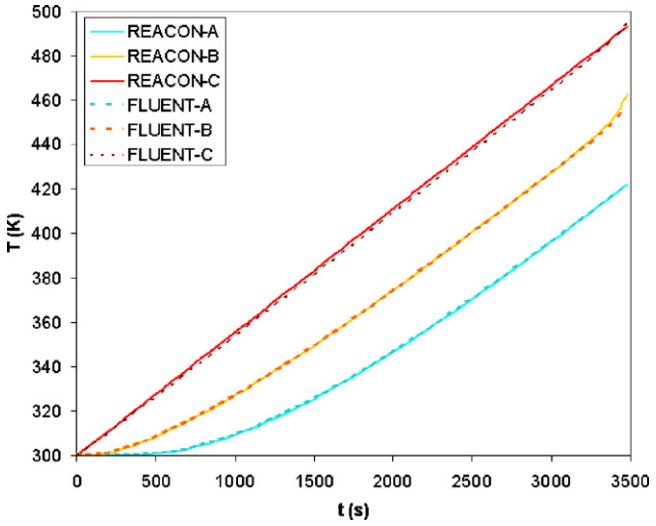

Fig. 2. Change of temperature values with time obtained by REACON and FLUENT codes at points A(0.05,0.00), B(0.05,0.02) and C(0.05,0.03).

that REACON code can be used for the 2D reactive conduction heat transfer computations for the simulation of the slow cook-off tests.

3. Simulation of a slow cook-off experiment

As mentioned in the previous sections, the purpose of the development of the REACON code is the simulation of cook-off tests and estimation of the ignition times, locations of ignition and temperatures in specified munitions. In Ref. [14], experimental results were obtained in terms of ignition time and ignition temperature for the slow cook-off of a generic warhead having PBXN-110 explosive enclosed in an aluminum case. The code was employed for the simulation of slow cook-off of this generic warhead. For this purpose, a finite element model of the generic test item was built. The boundary conditions to which the test item was exposed during the experiment were applied to this model and the estimation of the ignition time, location of ignition and the temperature gradient are obtained.

The generic warhead test item is cylindrical in shape and has a symmetry plane in the mid of the longitudinal direction in addition to the axial symmetry [14]. Therefore, a quarter model of the test

Table 2
Comparison of ignition times for 25.4 mm RDX sphere at constant temperature boundary conditions.

Surface temperature (°C)	Ignition time (s)			
	Zinn and Mader [3]	Anderson [5]	Suceska [6]	REACON-1D
180	1000	1030	1051.8	1056.1
200	420	458	466.9	467.9
220	120	162	166.1	167.1
240	33	42.9	44.0	44.4
260	10.5	10.1	10.3	10.6

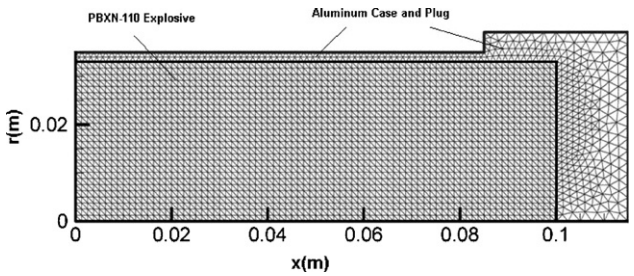

Fig. 3. The solution domain for the generic test item.

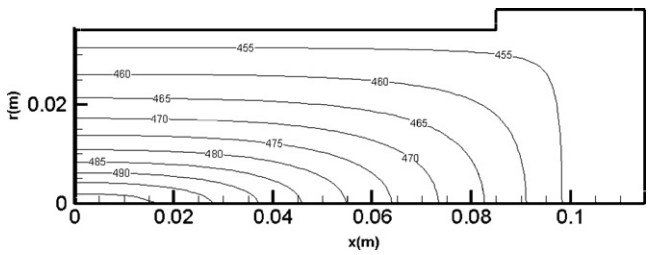

Fig. 4. The calculated temperature contours in Kelvin over the computation domain just after the ignition instance.

Table 4
Computational parameters and boundary and initial conditions for the computation of slow cook-off test item.

Parameters	REACON
Domain discretization	2-D axial symmetric finite element
Time discretization	Transient, Crank-Nicholson
Element type	Triangular, three nodes
Boundary conditions	Increasing surface temperature (5 K/h)
Initial conditions	410 K

item is created in order to decrease the total number of elements used in the computations. The solution domain for the computation is prepared with 2400 number of triangular elements and is shown in Fig. 3. Moreover, the computational parameters are presented in Table 4.

In order to determine the mesh and time step size sensitivity of the computation for this problem, computations with three different numbers of element and time step sizes were performed as presented in Tables 5 and 6. From the mesh and time step size sensitivity analysis, it was deduced that computations would be performed with 4975 number of elements and 5.0 s time step size, which resulted in less than 0.1% deviations from the most accurate case.

Typical temperature contours in the computation domain just after the ignition instances are provided in Fig. 4. As seen in this figure, the temperature distribution in the domain shows that maximum temperature occurs at the center, which also leads to the start of ignition at the center. The time to ignition t_{ign} starting from the heating instance, the ignition temperature T_{ign} which corresponds to the maximum temperature in the domain at the ignition instance, and the surface temperature outside the aluminum case at the ignition time $T_{surf,\text{-}ign}$ obtained from the simulation for the slow cook-off test are;

$$t_{ign} = 8.70\,\text{h} \quad T_{ign} = 470.0\,\text{K} \quad T_{surf,\text{-}ign} = 454.0\,\text{K}$$

Table 5
Ignition times and relative deviations for the computations with different numbers of elements.

Number of elements	Ignition time (s)	% Deviation
1370	30,100	0.23
4975	30,060	0.10
8225	30,030	0.00

Table 6
Ignition times and relative deviations for the computations with different time step sizes.

Time step size (s)	Ignition time (s)	% Deviation
1.0	29,953	0.00
5.0	29,970	0.06
10.0	30,000	0.16

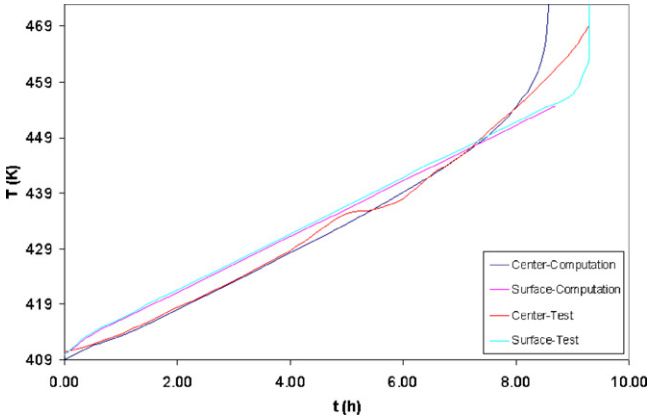

Fig. 5. Center and surface temperatures obtained from the experiment [14] and the simulation.

As explained in Section 2.2, it is assumed that the ignition takes place at the time step which corresponds to a 5% larger temperature increase rate from the previous time step.

The center and the surface temperature change in time obtained from the experiment [14] and the simulation are plotted as shown in Fig. 5. As seen in time history of the temperature values, a good agreement between the test and the computation results is observed. A quantitative comparison of the ignition temperatures and the surface temperatures at the ignition occurrence can be done using the results given in Table 7. When the values shown in Table 7 are examined, it is seen that there is a good agreement with a maximum of 7% deviation between the test and computation results in terms of the ignition time, the ignition temperature and the surface temperature when the ignition occurred.

4. Parametric computational study

In order to determine the effect of sample size and heating rate on the ignition time and the ignition location of the explosive material, several computations were performed. In order to determine the effect of size, eight domains scaled in size were employed with 5 K/h heating rate. Similarly, simulations were performed for six different boundary conditions with different heating rates for 70 mm diameter cylindrical sample. The change of ignition times with diameter of samples is given in Fig. 6. As seen in this figure, the ignition time decreases with increasing size up to 100 mm diam-

Table 7
Comparison of ignition times and surface temperatures at ignition.

Results	Test	Computation	% Difference
Ignition time (h)	9.31	8.70	6.55
Ignition temperature (K)	469.5	470	0.11
Surface temperature at ignition (K)	462.5	454.0	1.84

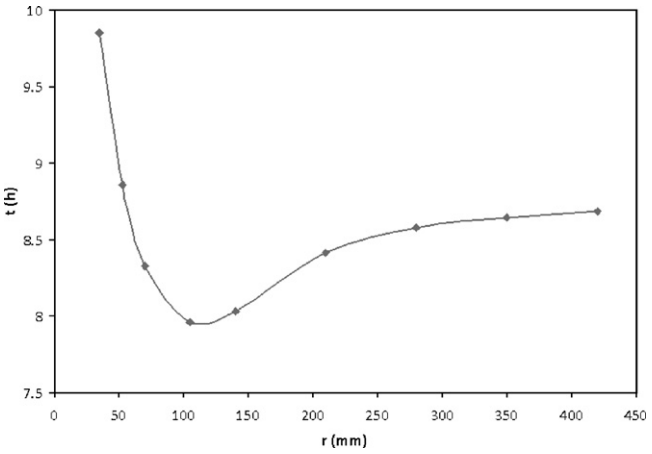

Fig. 6. Ignition times for samples with different sizes.

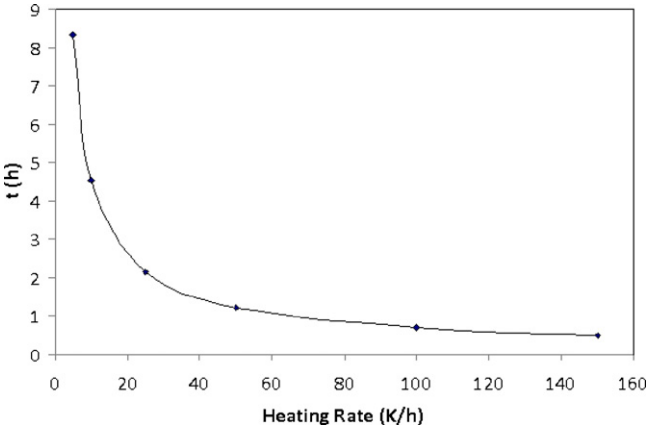

Fig. 7. The change of ignition time with heating rate.

eter. However, it is observed that for the samples with diameters larger than 100 mm, the ignition time increases with increasing size and converges to a value around 8.5 for very large samples. From the results of the computations it is also noticed that the ignition locations for samples with diameters smaller than 100 mm are close to the center of the samples while they are close to the surface for large ones. This phenomenon can be explained by the low conductance of the explosive material and the change of area to volume ratio. For small samples the heat generated inside can be dissipated out faster due to the larger area to volume ratio which results in increase in the ignition time. However, for very large samples heat supplied from outside cannot diffuse to the center up to the ignition occurrence and the total amount of necessary heat is larger which results in increase in the ignition time.

Similarly, the ignition times of the 70-mm diameter cylindrical explosive sample for different heating rates are given in Fig. 7. As seen in Fig. 7, the ignition time for the explosive material decreases with increasing heating rate. Moreover, the ignition occurs at a location close to the surface of the sample with high heating rates while it is at the center for low heating rates.

5. Conclusion

In the scope of this study, a code named REACON is developed in order to perform 2D reactive conduction analysis for the models of the munitions to be designed against cook-off stimuli. The validation of the code results was performed with comparison to the data in the literature and the results obtained by a commercial code. REACON enables the prediction of the temperature distribution throughout a munition and the ignition location and time of the energetic material under certain surrounding conditions. For the specified slow cook-off experimental conditions, the ignition temperature and time to ignition of the energetic material were calculated and shown to be in good agreement with a deviation of 7% from the experimental condition. These predictions are important in terms of the insensitive munitions design procedure and taking precautions when such an accidental event occurs in the operational field. Additionally, a parametric study was performed showing the effect of dimensional scaling and the heating rate on the ignition characteristics. It was shown that at relatively small munition size, ignition occurs later and the minimum ignition time was obtained at around 100 mm radius for the specified munition geometry. At larger munition size, the ignition time levels off around 8.5 h. Similarly, the inverse proportional effect of the heating rate on the ignition time was shown for the baseline munition geometry which depicts the transition from fast cook-off to slow cook-off experimental conditions.

Acknowledgements

We would like to thank TÜBİTAK-SAGE (The Scientific and Technological Research Council of Turkey – Defense Industries Research and Development Institute) for supporting this work.

References

[1] N.N. Semenov, Theories of combustion process, Z. fur Physik. 48 (1928) 571–582.
[2] D.A. Frank-Kamenetskii, Calculation of thermal explosion limits, Acta Physiochim. URSS 10 (1939) 365–370.
[3] J. Zinn, C.L. Mader, Thermal initiation of explosives, J. Appl. Phys. 31 (1960) 323–328.
[4] G. Merzhanov, V.G. Abramov, Thermal explosion of explosives and propellants: a review, Propell. Explos. Pyrotech. 6 (1981) 130–148.
[5] A. Anderson, TEPLO – a heat conduction code for studying thermal explosion in laminar composites LA-4511, Los Alamos Scientific Laboratory, Los Alamos, 1970.
[6] M. Suceska, A computer program based on finite difference method for studying thermal initiation of explosives, J. Therm. Anal. Calorim. 68 (2002) 865–875.
[7] Suceska M., Influence of thermal decomposition kinetic model on results of propellants self-ignition numerical modeling, in: Proceedings of the 5th New Trends in Research of Energetic Materials, Pardubice, Czech Republic, April 24–25, 2002, pp. 309–322.
[8] M. Suceska, S. Matecic-Musanic, Numerical modeling of self-ignition of energetic materials, Central Eur. J. Energ. Mater. 1 (2004) 23–42.
[9] Z.Y. Liu, M. Suceska, Numerical prediction on cookoff explosion of explosive under strong confinement, in: S. Itoh, K. Hokamoto (Eds.), Explosion, Shock Wave, and Hypervelocity Phenomena in Materials II, Materials Science Forum, 2008, pp. 89–94.
[10] J. Isler, D. Kayser, Correlation between kinetic properties and self-ignition of nitrocellulose, in: Proc. of the 6th Symp. Chem. Probl. Connected Stab. Explos, Kungalav, Sweden, 1982, pp. 217–237.
[11] R.R. McGuire, C.M. Tarver, Chemical decomposition models for thermal explosion of confined HMX, RDX, and TNT explosives UCRL-84986, Lawrence Livermore Laboratory, Livermore, 1981.
[12] C.M. Tarver, T.D. Tran, Thermal decomposition models for HMX-based plastic bonded explosives, Combust. Flame 137 (2004) 50–62.
[13] www.fluent.com (accessed 23.05.10).
[14] E. Aydemir, A. Ulas, N. Serin, Experimental investigation of cook-off of munitions, in: ISEM the 3rd International Symposium on Energetic Materials and Their Applications, Tokyo, Japan, 2008.